Magnetic and vortical impacts on the effective QCD phase diagram

Luis Alberto Hernández Rosas
Universidad Autónoma Metropolitana

Eur.Phys.J.A 57 (2021) 7
ArXiv:2410.17874

The 7th International Conference on Particle Physics and Astrophysics
Moscow, Russia, October 25th 2024

CONTENT

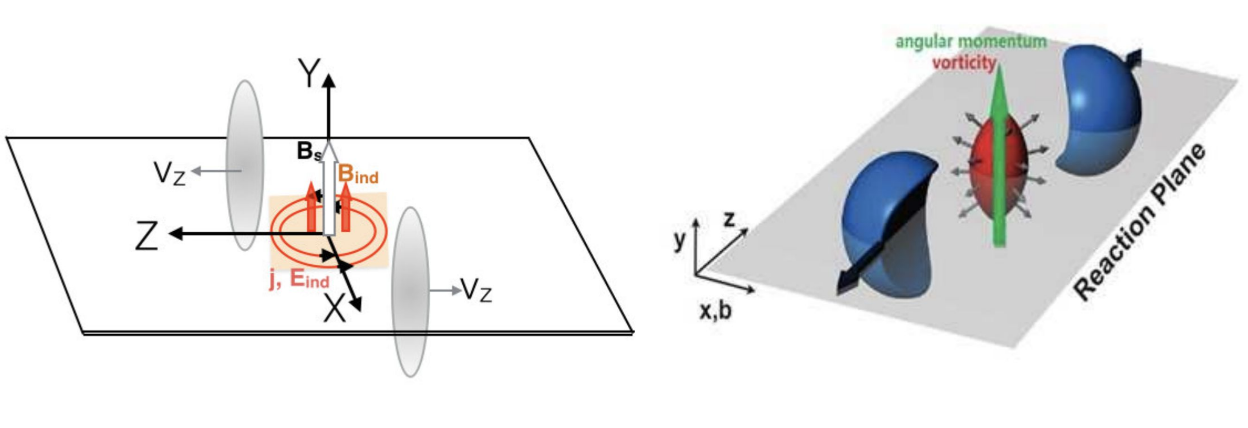

- PHYSICS MOTIVATION
- LSMq AND THE EFFECTIVE POTENTIAL
- PHASE DIAGRAM, CEP AND FINAL REMARKS

HIC

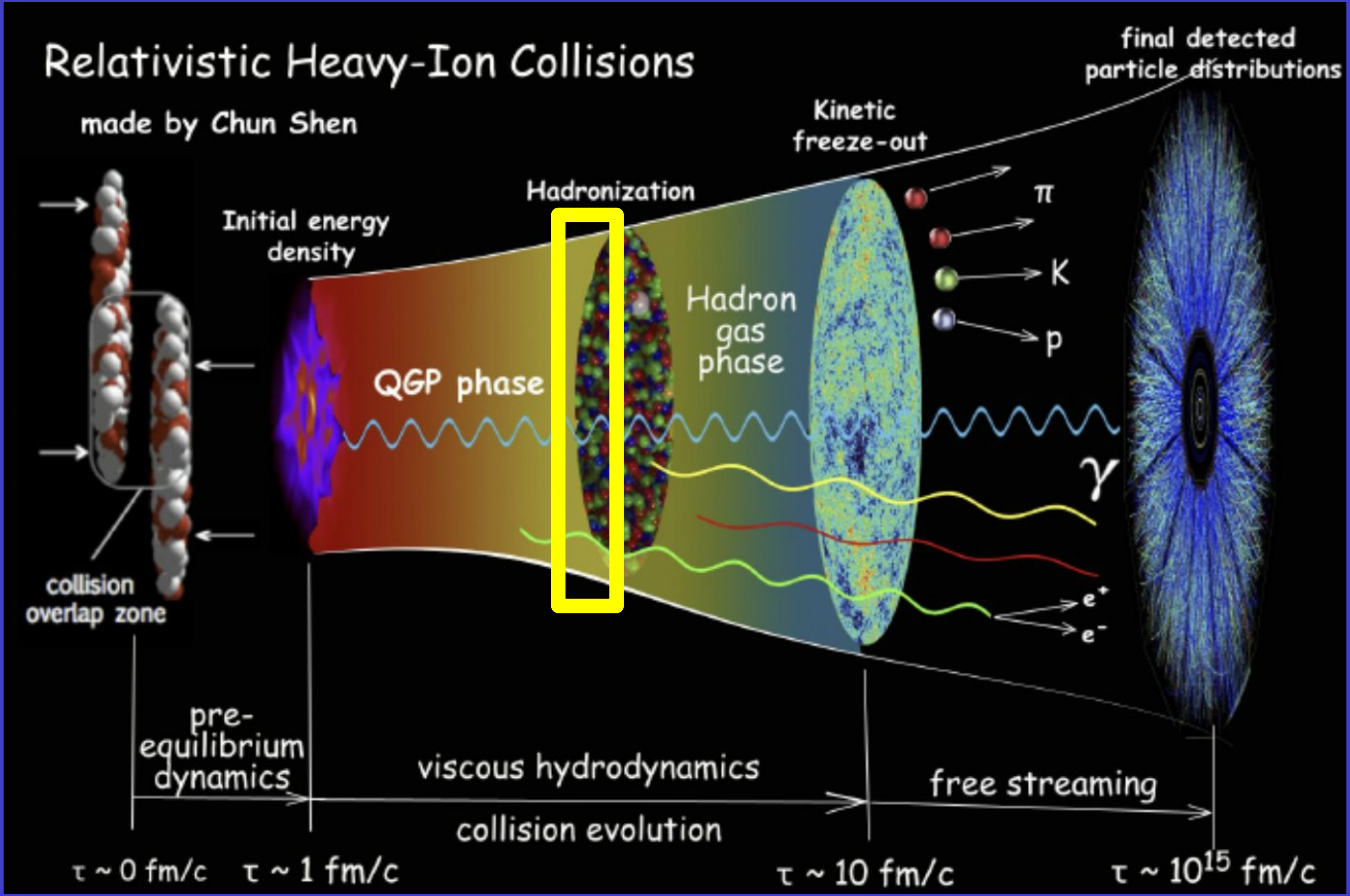
Relativistic Heavy-Ion Collisions
made by Chun Shen
final detected particle distributions
Kinetic freeze-out
Hadronization
Initial energy density
QGP phase
Hadron gas phase
π
K
p
γ
e⁺
e⁻
collision overlap zone
pre-equilibrium dynamics
viscous hydrodynamics
free streaming
collision evolution
τ ~ 0 fm/c
τ ~ 1 fm/c
τ ~ 10 fm/c
τ ~ 10^15 fm/c

NON CENTRAL COLISION

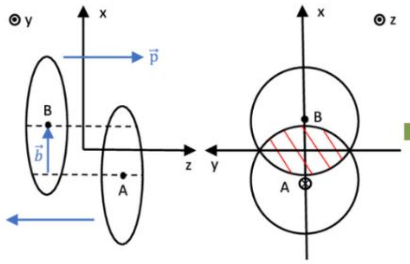

Eur.Phys.J.C 83 (2023) 1, 96

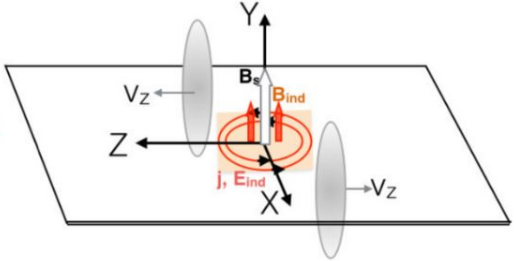

Phys.Rev.C 96 (2017) 5, 054909

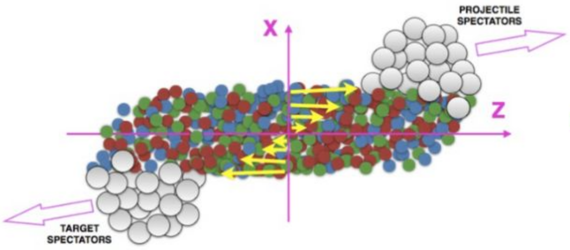

EPJ Web Conf. 171 (2018) 07002

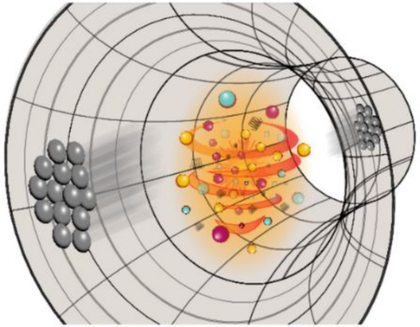

Nucl.Sci.Tech. 34 (2023) 1, 15

ANGULAR VELOCITY

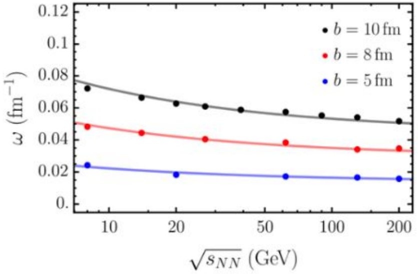

Initial angular velocity ω for Au + Au collisions at impact parameters b= 5, 8, 10 fm as functions of collision energy (UrQMD). Phys. Rev. D **102** (2020), 056019

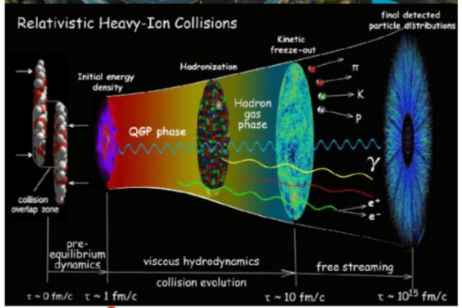

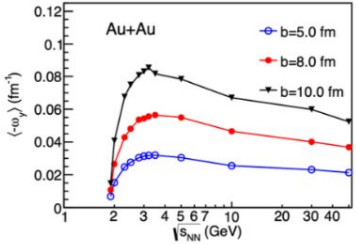

Initial angular velocity at mid rapidity as a function of the collision energy for impact parameters b = 5, 8, and 10 fm (UrQMD). Phys.Rev.C **101** (2020) 6, 064908

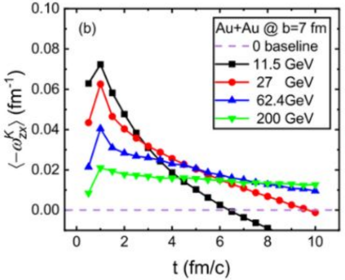

Time evolution of angular velocity at b=7 fm and four different energies (PACIAE). Phys.Rev.C **104** (2021) 5, 054903

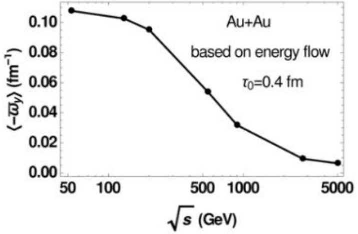

Angular velocity at fixed τ = 0.4 fm and η = 0 as function of collision energy (HIJING). Phys. Rev. C **93** (2016), 064907

MAGNETIC FIELDS

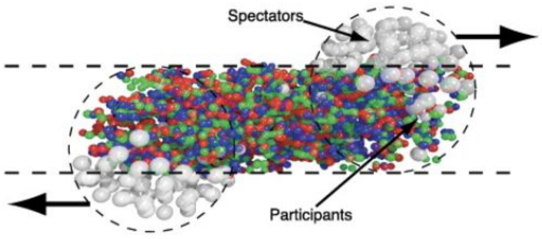

R. Snellings, J. Phys. **13**, (2011) 055008

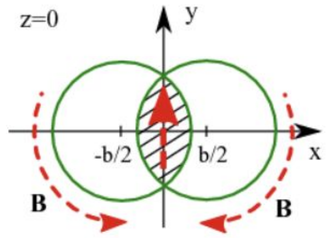

V. Voronyuk *et al.*,Phys. Rev. C **83**, 054911 (2011)

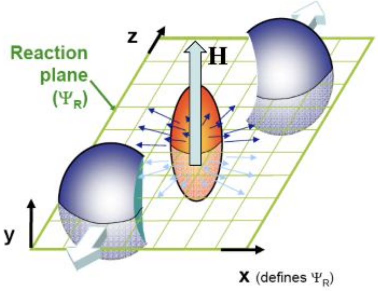

D. E. Kharzeev, L. D. McLerran and H. J. Warringa, Nucl. Phys. A **803**, 227 (2008)

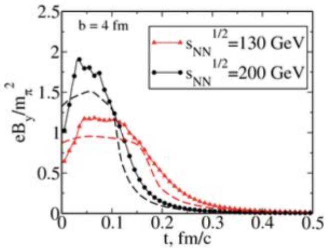

V. Skokov, A. Y. Illarionov and V. Toneev, Int. J. Mod. Phys. A **24**, 5925 (2009)

HICs

1. **Phase transition**
   Quark-Gluon Plasma → Chiral Symmetry

2. **Non-central collisions**
   Finite Impact Parameter **b**

3. **Angular velocity**
   Maximum value ~0.1 fm^{-1} (~20 MeV)

4. **Magnetic Fields**
   Short pulse with maximum high ~ $(m_\pi)^2$

5. **Collision Energy**
   Effects more important at low energies

6. **Baryon Chemical Potential**
   Region of maximum baryon density (MPD-NICA)

7. **Effective models**
   Low energies of QCD

QCD phase diagram

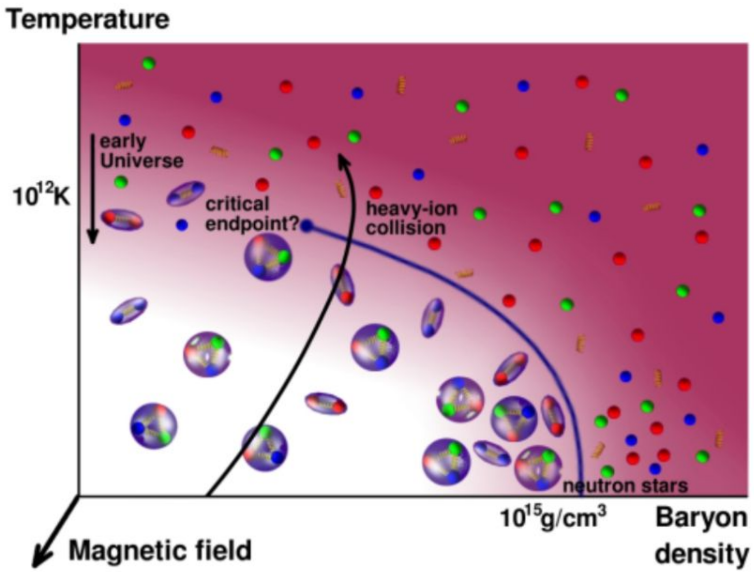

J.Phys.Conf.Ser. 503 (2014) 012009

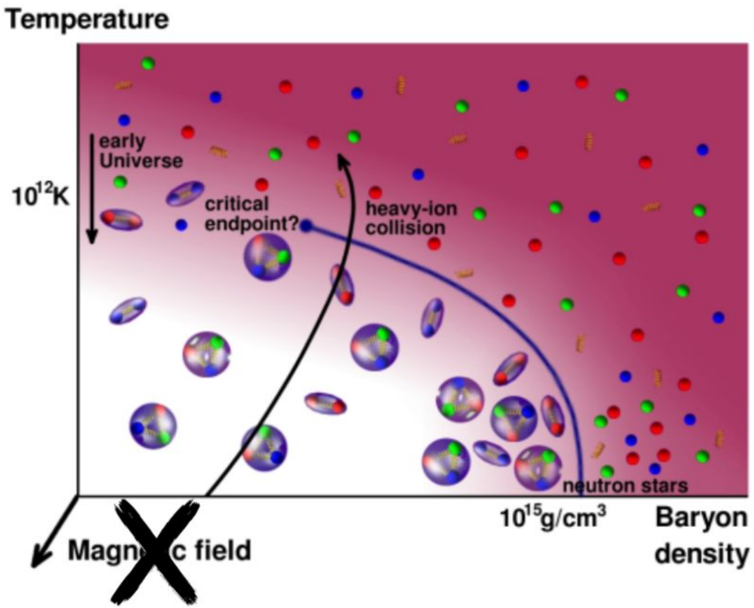

Vorticity

QCD phase diagram

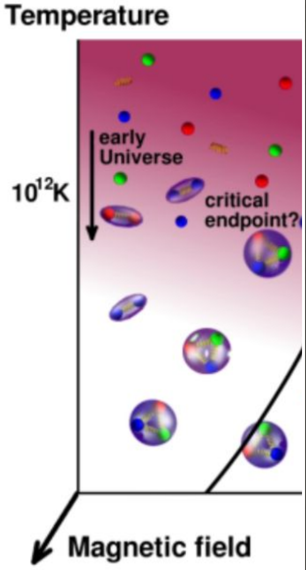

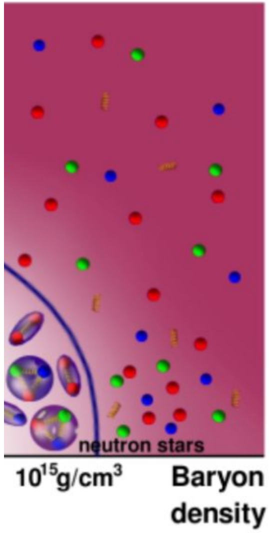

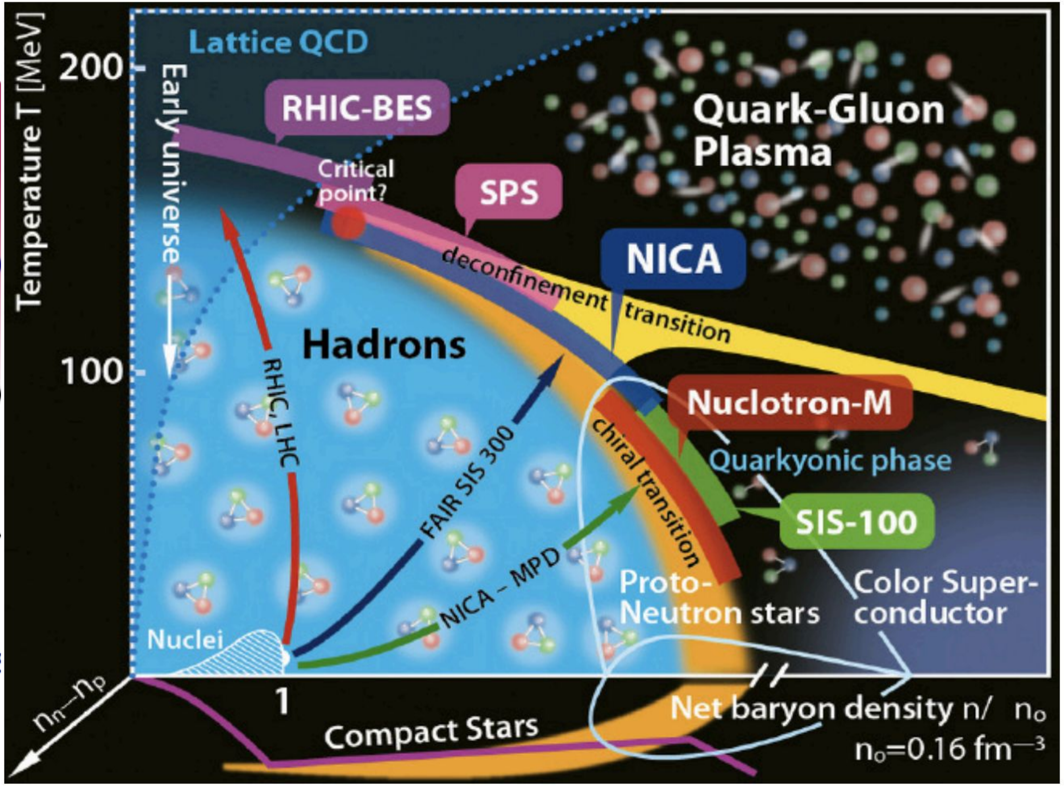

J.Phys.Conf.S

Linear Sigma model coupled to quarks

Effective theory which is usefull to emulate the low energy regime of Quantum Chromodynamics. It exhibits a symmetry spontaneously broken.

$$\mathscr{L} = \frac{1}{2}(\partial_\mu \sigma)^2 + \frac{1}{2}(\partial_\mu \vec{\pi})^2 + \frac{a^2}{2}(\sigma^2 + \vec{\pi}) - \frac{\lambda}{4}(\sigma^2 + \vec{\pi}^2)^2 + i\bar{\psi}\gamma^\mu \partial_\mu \psi - ig\bar{\psi}\gamma^5 \vec{\tau}.\vec{\pi}\psi - g\bar{\psi}\psi\sigma$$

letting the sigma-field to develop a vacuum expectation value v, we have

$$V^{tree} = -\frac{a^2}{2}v^2 + \frac{\lambda}{4}v^4$$

$$\sigma \to \sigma + v$$

$$m_\sigma^2 = 3\lambda v^2 - a^2 \quad , \quad m_0^2 = \lambda v^2 - a^2 \quad , \quad m_f = gv$$

$$a^2, \lambda, g$$

CHIRAL SYMMETRY RESTORATION

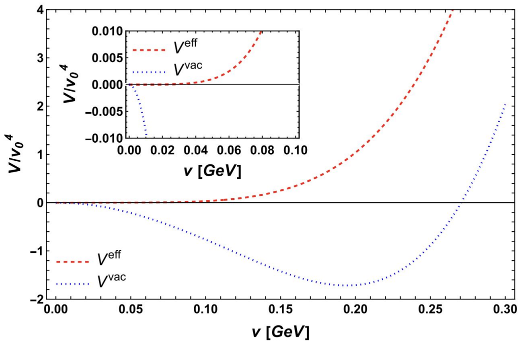

v= vacuum expectation value → order parameter

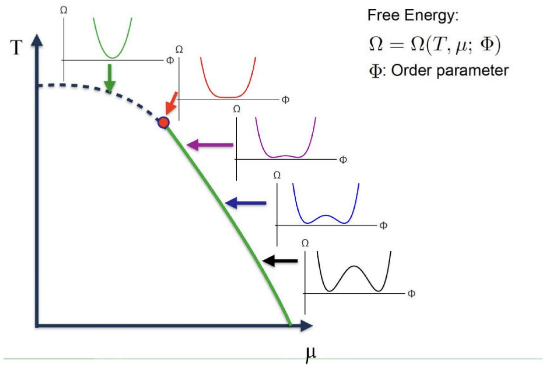

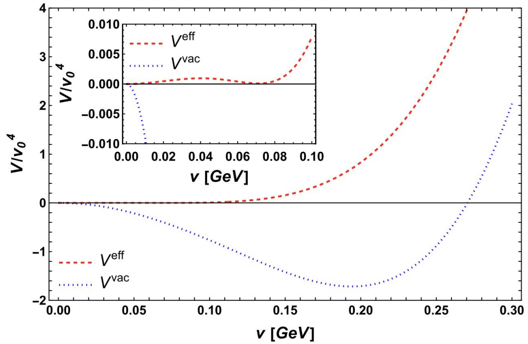

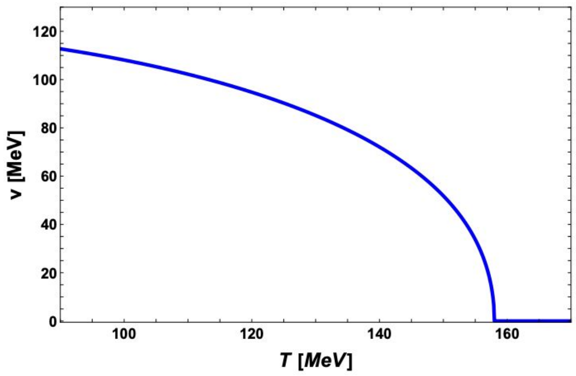

low ← μ_q → high

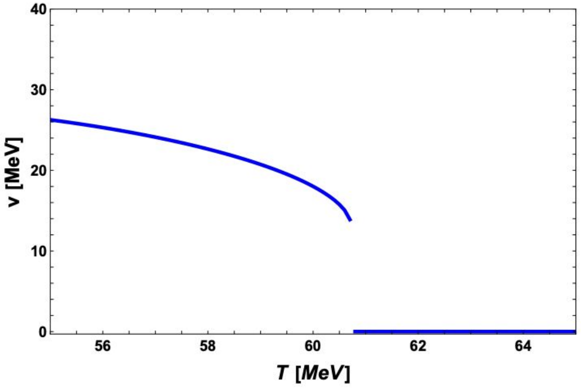

EFFECTIVE POTENTIAL

$$V^{\text{eff}} = V^{\text{tree}} + V_b^1 + V_f^1 + V^{\text{rings}}$$

$$V_b^1 = -\frac{i}{2}\int \frac{d^4k}{(2\pi)^4}\ln(D_b^{-1}(k)) \;,\; V_f^1 = iN_c \int \frac{d^4k}{(2\pi)^4} Tr[\ln(S_f^{-1}(k))]$$

$$V^{\text{ring}} = \frac{T}{2}\sum_{n=-\infty}^{\infty}\int \frac{d^3k}{(2\pi)^3}\ln\left(1+\Pi D(\omega_n,\Omega,\vec{k})\right),$$

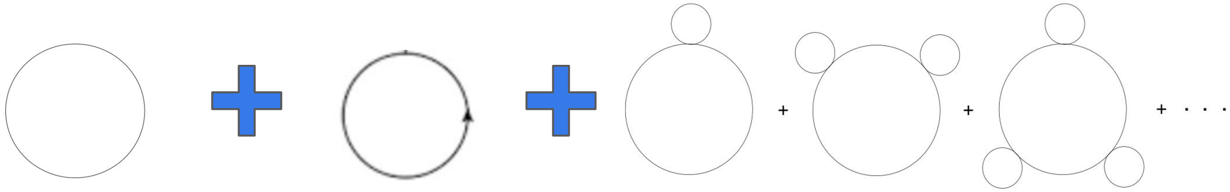

PROPAGATORS

Finite **eB**

Boson

$$D(p) \;=\; \int_0^\infty \frac{ds}{\cos(|q_b B|s)} e^{is\left(p_\parallel^2 - p_\perp^2 \frac{\tan(|q_b B|s)}{|q_b B|s} - m_b^2 + i\epsilon\right)},$$

Phys.Rev.D 108 (2023) 9, 094020

Fermion

$$\begin{aligned} S_f(p) \;&=\; \int_0^\infty \frac{ds}{\cos(|q_f B|s)} e^{is\left(p_\parallel^2 - p_\perp^2 \frac{\tan(|q_f B|s)}{|q_f B|s} - m_f^2 + i\epsilon\right)} \\ &\times \left[\left(\cos(|q_f B|s) + \gamma_1\gamma_2 \sin(|q_f B|s)\mathrm{sign}(q_f B)\right)\right. \\ &\times \left.\left(m_f + \not{p}_\parallel\right) - \frac{\not{p}_\perp}{\cos(|q_f B|s)}\right], \end{aligned}$$

Phys.Rev.D 103 (2021) 7, 076021

Finite **Ω**

Boson

$$D(p) = \frac{1}{(p_0 + \Omega)^2 - p_\perp^2 - p_z^2 - m^2 + i\epsilon}$$

Fermion

$$\begin{aligned} S(p) = &\frac{(p_0 + \Omega/2 - p_z + ip_\perp)(\gamma_0 + \gamma_3) + m(1 + \gamma_5)}{(p_0 + \Omega/2)^2 - \bar{p}^2 - m^2 + i\epsilon}\mathcal{O}^+ \\ + &\frac{(p_0 - \Omega/2 + p_z - ip_\perp)(\gamma_0 - \gamma_3) + m(1 + \gamma_5)}{(p_o - \Omega/2)^2 - \bar{p}^2 - m^2 + i\epsilon}\mathcal{O}^-, \end{aligned}$$

Phys.Rev. 82 (1951) 664-679

EFFECTIVE POTENTIAL Ω

$$V^{\rm eff} = -\frac{a^2}{2}v^2 + \frac{\lambda}{4}v^4 + \sum_{b=\sigma,\vec{\pi}} \left\{ -\frac{m_b^4}{64\pi^2}\left[\ln\left(\frac{\mu^2}{16\pi^2T^2}\right) + 2\gamma_E\right] - \frac{\pi^2T^4}{90} + \frac{T^2}{24}\left(m_b^2 - 2\Omega^2\right) - \frac{T\left(\Pi + m_b^2 - \Omega^2\right)^{3/2}}{12\pi} - \frac{\Omega^2}{48\pi^2}\left(3m_b^2 - \Omega^2\right) \right\}$$

$$+ N_f N_c \left\{ \frac{m_f^4}{16\pi^2}\left[\ln\left(\frac{\mu^2}{\pi^2T^2}\right) + 2\gamma_E - \frac{3}{4}\right] - \frac{7T^4\pi^2}{180} - \frac{T^2}{12}\left(\left(\mu_q + \frac{\Omega}{2}\right)^2 + \left(\mu_q - \frac{\Omega}{2}\right)^2\right) - \frac{T^2m_f^2}{4\pi^2}\left(\mathrm{Li}_2\left(-e^{\frac{\mu+\frac{\Omega}{2}}{T}}\right) + \mathrm{Li}_2\left(-e^{\frac{\mu-\frac{\Omega}{2}}{T}}\right) + \mathrm{Li}_2\left(-e^{-\frac{\mu+\frac{\Omega}{2}}{T}}\right) + \mathrm{Li}_2\left(-e^{-\frac{\mu-\frac{\Omega}{2}}{T}}\right)\right) - \frac{\left(\mu+\frac{\Omega}{2}\right)^4 + \left(\mu-\frac{\Omega}{2}\right)^4}{24\pi^2} \right\}.$$

- Imaginary time formalism for TFT.
- Finite T, **μ_q** and **Ω**
- High T approximation.
- Ring diagramas → Screening effects.

$$\Pi = \frac{\lambda T^2}{2} - \frac{N_f N_c T^2 g^2}{2\pi^2}\left(\mathrm{Li}_2\left(-e^{\frac{\mu+\frac{\Omega}{2}}{T}}\right) + \mathrm{Li}_2\left(-e^{\frac{\mu-\frac{\Omega}{2}}{T}}\right) + \mathrm{Li}_2\left(-e^{-\frac{\mu+\frac{\Omega}{2}}{T}}\right) + \mathrm{Li}_2\left(-e^{-\frac{\mu-\frac{\Omega}{2}}{T}}\right)\right).$$

EFFECTIVE POTENTIAL eB

$$
\begin{aligned}
V^{(eff)} &= -\frac{a^2}{2}\left\{1+\frac{3a^2}{8\pi^2}\left[\lambda\ln\left(\frac{2a^2}{\tilde{\mu}^2}\right)-8\frac{g^4}{\lambda}+2\lambda\right]\right\}v^2 \\
&+\frac{\lambda}{4}\left\{1+\frac{3}{4\pi^2}\left[8g^4\ln\left(\frac{g^2a^2}{\lambda\tilde{\mu}^2}\right)-3\lambda^2\ln\left(\frac{2a^2}{\tilde{\mu}^2}\right)\right]\right\}v^4 \\
&+\sum_{b=\pi^\pm,\pi^0,\sigma}\left\{-\frac{T^4\pi^2}{90}+\frac{T^2m_b^2}{24}-\frac{T(m_b^2+\Pi_b)^{3/2}}{12\pi}-\frac{m_b^4}{64\pi^2}\left[\ln\left(\frac{\tilde{\mu}^2}{(4\pi T)^2}\right)+2\gamma_E\right]\right\} \\
&-\frac{|q_bB|^2}{24\pi^2}\sum_{b=\pi^\pm}\left\{\frac{T\pi}{2(m_b^2+\Pi_b)^{1/2}}+\frac{1}{4}\ln\left(\frac{\tilde{\mu}^2}{(4\pi T)^2}\right)+\frac{1}{2}\gamma_E\right. \\
&\left.-\frac{1}{4}\zeta(3)\left(\frac{m_b^2}{(2\pi T)^2}\right)+\frac{3}{16}\zeta(5)\left(\frac{m_b^4}{(2\pi T)^4}\right)\right\} \\
&+N_cN_f\left\{\frac{m_f^4}{16\pi^2}\left[\ln\left(\frac{\tilde{\mu}^2}{T^2}\right)-\psi^0\left(\frac{1}{2}+\frac{i\mu}{2\pi T}\right)-\psi^0\left(\frac{1}{2}-\frac{i\mu}{2\pi T}\right)\right.\right. \\
&\left.+\psi^0\left(\frac{3}{2}\right)-2\left(1+\ln(2\pi)\right)+\gamma_E\right] \\
&-\frac{m_f^2T^2}{2\pi^2}\left[\mathrm{Li}_2\left(-e^{-\frac{\mu}{T}}\right)+\mathrm{Li}_2\left(-e^{\frac{\mu}{T}}\right)\right]+\frac{T^4}{\pi^2}\left[\mathrm{Li}_4\left(-e^{-\frac{\mu}{T}}\right)+\mathrm{Li}_4\left(-e^{\frac{\mu}{T}}\right)\right] \\
&+\frac{|q_fB|^2}{12\pi^2}\left(\frac{1}{2}\ln\left(\frac{\tilde{\mu}^2}{4\pi^2T^2}\right)+\frac{1}{2}\psi^0\left(\frac{1}{2}+\frac{i\mu}{2\pi T}\right)+\frac{1}{2}\psi^0\left(\frac{1}{2}-\frac{i\mu}{2\pi T}\right)\right. \\
&\left.\left.+\frac{1}{2}\psi^0\left(\frac{1}{2}\right)-2\ln(2\pi)+\gamma_E-\frac{m_f^2}{16\pi^2T^2}\left[\zeta\left(3,\frac{1}{2}+\frac{i\mu}{2\pi T}\right)+\zeta\left(3,\frac{1}{2}-\frac{i\mu}{2\pi T}\right)\right]\right)\right\},
\end{aligned}
$$

- Imaginary time formalism for TFT.
- Finite T, μ_q and eB.
- High T approximation.
- Weak eB field approximation.
- Ring diagramas → Screening effects.

$$
\Pi_b=\lambda\frac{T^2}{2}-N_fN_cg^2\frac{T^2}{\pi^2}\left[\mathrm{Li}_2\left(-e^{-\frac{\mu}{T}}\right)+\mathrm{Li}_2\left(-e^{\frac{\mu}{T}}\right)\right]
$$

PHASE DIAGRAM Ω

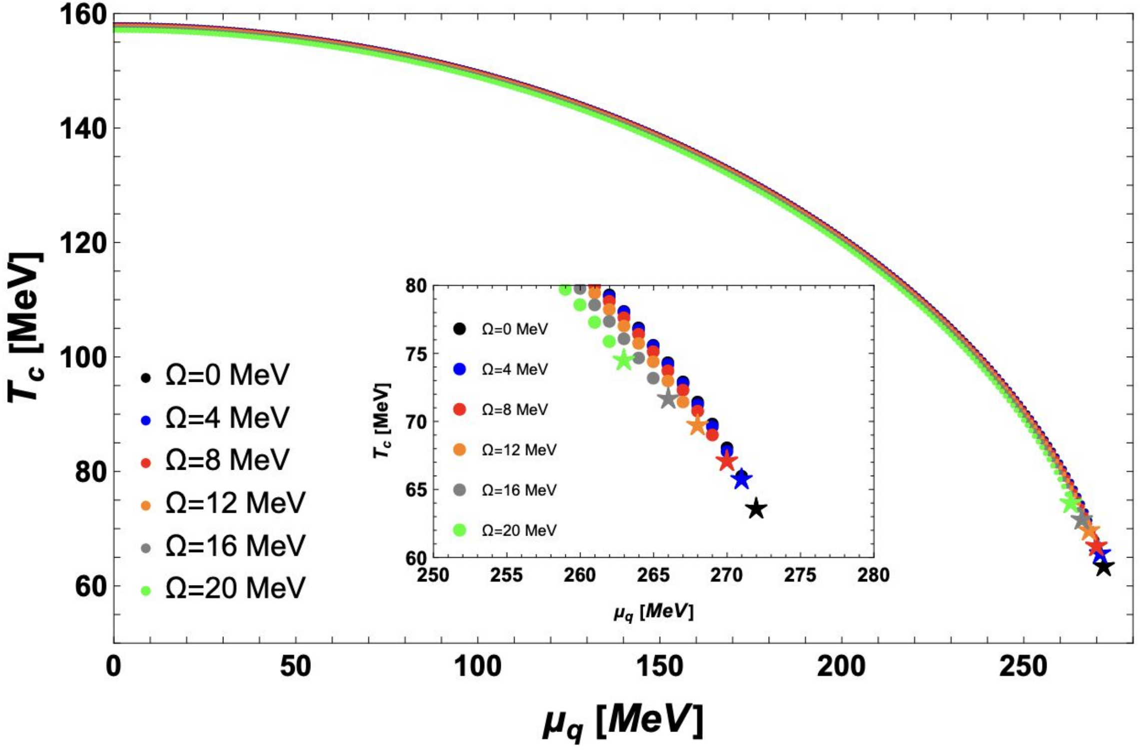

- The $\mathbf{T_c}$ decreases as the **Ω** increases.
- Larger **Ω** moves the CEP to lower $\boldsymbol{\mu_q}$ and higher T.
- The **Ω** not only modifies the conditions under which the phase transition occurs, but also the nature of the transition

PHASE DIAGRAM eB

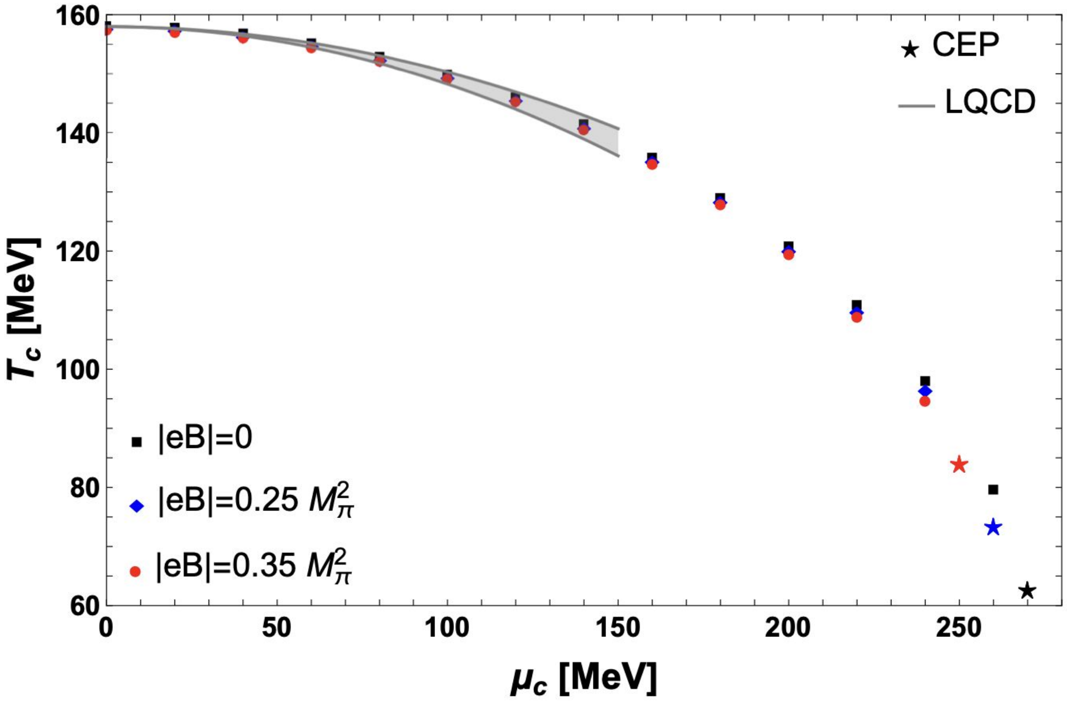

- The $\mathbf{T_c}$ decreases as the **eB** increases.
- Larger **eB** moves the CEP to lower $\boldsymbol{\mu}_q$ and higher T.
- The **eB** not only modifies the conditions under which the phase transition occurs, but also the nature of the transition

PHASE DIAGRAMS

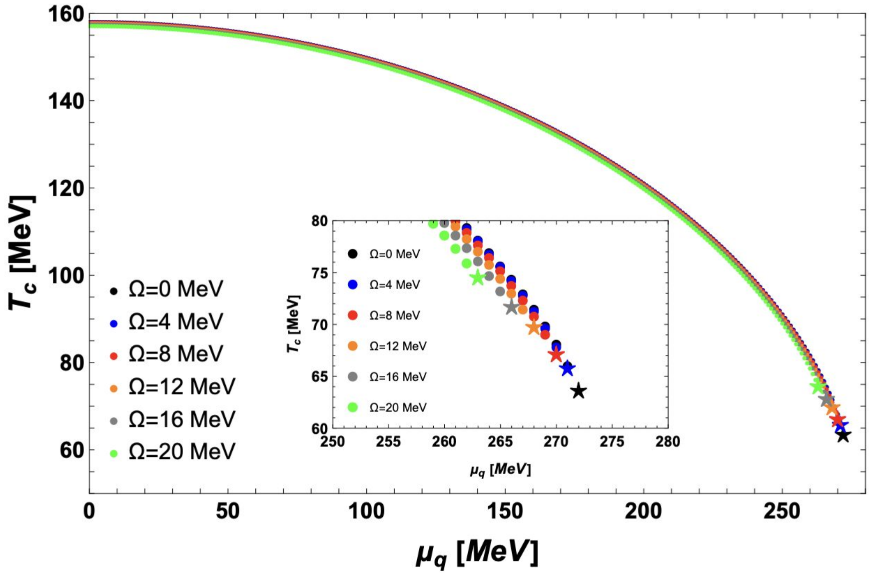

a=148.7 MeV, λ=1.4 and g=0.88

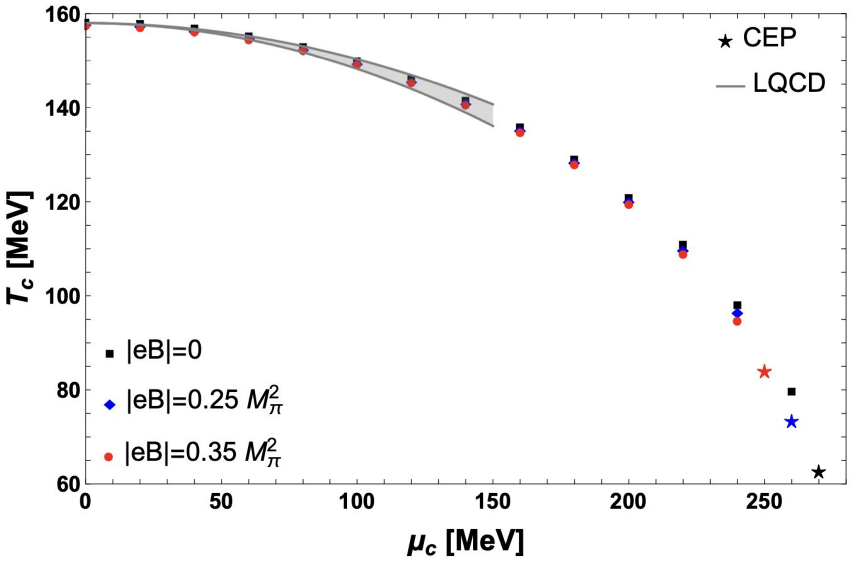

a=133.5 MeV, λ=1.6 and g=0.79

SUMMARY

- **Ω and eB promote the chiral symmetry restoration.**
- **Significant changes in the position of the CEP as a function of Ω or eB**
- Computation of the low T approximation
- Enough equations to fix the free parameters
- Put together **Ω and eB**

Thanks for your attention!

lhernandez.rosas@izt.uam.mx
luis.hr@xanum.uam.mx

BARYON NUMBER FLUCTUATION

Conserved Charges: Net Baryon Number (B), Net Charge (Q), Net Strangeness (S)

Measured multiplicity N, $\langle \delta N \rangle = \mathbf{N} - \langle N \rangle$

$$\text{mean:} \quad M = \langle N \rangle = C_1$$

$$\text{variance:} \quad \sigma^2 = \langle (\delta N)^2 \rangle = C_2$$

$$\text{skewness:} \quad S = \langle (\delta N)^3 \rangle / \sigma^3 = C_3 / C_2^{3/2}$$

$$\text{kurtosis:} \quad \kappa = \langle (\delta N)^4 \rangle / \sigma^4 - 3 = C_4 / C_2^2$$

Moments, cumulants and susceptibilities:

$$2^{nd} \text{ order:} \quad \sigma^2/M \equiv C_2/C_1 = \chi_2/\chi_1$$

$$3^{rd} \text{ order:} \quad S\sigma \equiv C_3/C_2 = \chi_3/\chi_2$$

$$4^{th} \text{ order:} \quad \kappa\sigma^2 \equiv C_4/C_2 = \chi_4/\chi_2$$

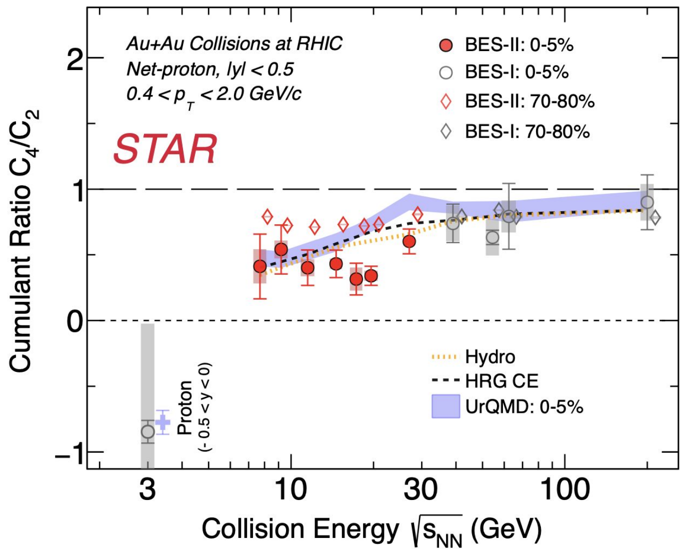

A. Pandav (STAR collaboration), plenary talk at CPOD 2024,
https:// conferences.lbl.gov/event/1376/contributions/8772/

BARYON NUMBER FLUCTUATION

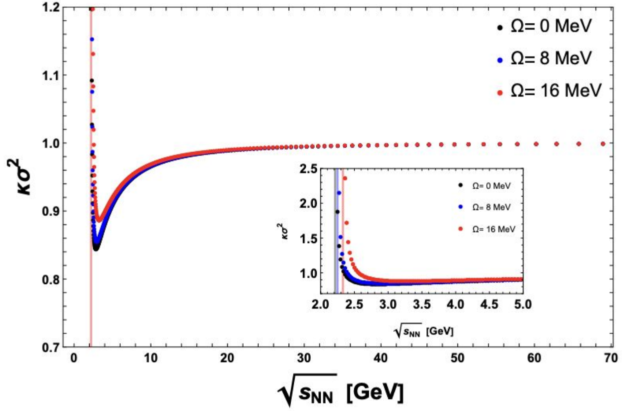

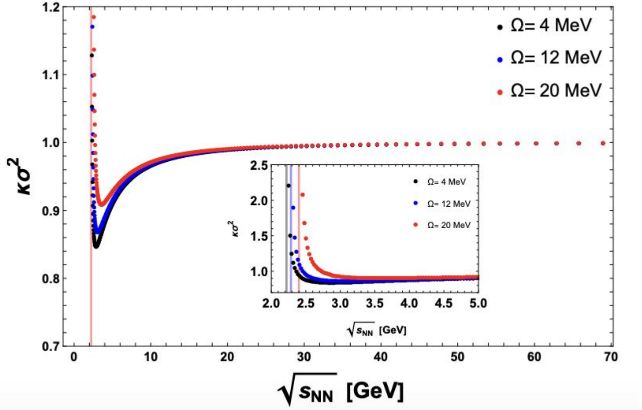

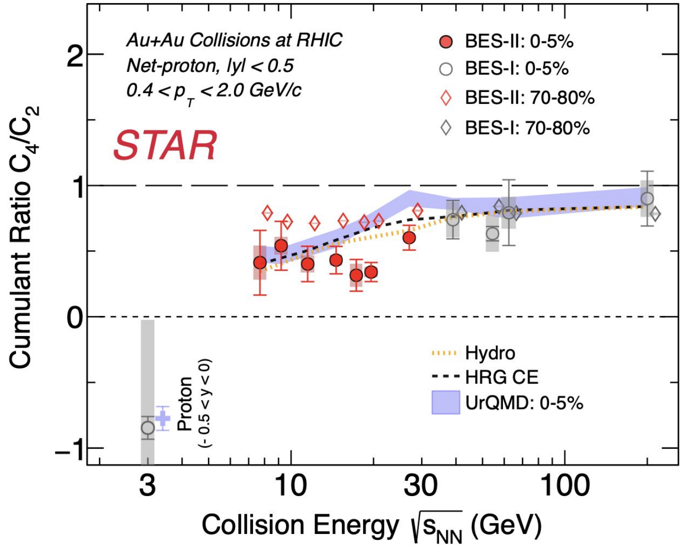

A. Pandav (STAR collaboration), plenary talk at CPOD 2024, https:// conferences.lbl.gov/event/1376/contributions/8772/

SUMMARY 2.0

- As the energy approaches the CEP position, the fourth moment exhibits a sharp increase, suggesting that the CEP location can be identified by this abrupt rise. This behavior is also influenced by vorticity, as higher values of Ω shift the CEP to higher collision energies.